Molecular Therapy
Original Article

A differentiated β-globin gene replacement strategy uses heterologous introns to restore physiological expression

Kirby A. Wallace,[1,2] Trevor L. Gerstenberg,[1] Craig L. Ennis,[1] Juan A. Perez-Bermejo,[1] James R. Partridge,[1] Christopher Bandoro,[1] William M. Matern,[1] Gaia Andreoletti,[1] Kristina Krassovsky,[1] Shaheen Kabir,[1] Cassandra D. Lalisan,[1] Aishwarya R. Churi,[1] Glen M. Chew,[1] Lana Corbo,[1] Jon E. Vincelette,[1] Timothy D. Klasson,[1] Brian J. Silva,[1] Yuri G. Strukov,[1] B. Joy Quejarro,[1] Kaisle A. Hill,[1] Sebastian Treusch,[1] Jane L. Grogan,[1] Daniel P. Dever,[1] Matthew H. Porteus,[2] and Beeke Wienert[1]

[1]Graphite Bio, Inc., South San Francisco, CA 94080, USA; [2]Kamau Therapeutics, Inc., South San Francisco, CA 94080, USA

β-Hemoglobinopathies are common monogenic disorders. In sickle cell disease (SCD), a single mutation in the β-globin (*HBB*) gene results in dysfunctional hemoglobin protein, while in β-thalassemia, over 300 mutations distributed across the gene reduce β-globin levels and cause severe anemia. Genetic engineering replacing the whole *HBB* gene through homology-directed repair (HDR) is an ideal strategy to restore a benign genotype and rescue *HBB* expression for most genotypes. However, this is technically challenging because (1) the insert must not be homologous to the endogenous gene and (2) synonymous codon-optimized, intron-less sequences may not reconstitute adequate β-globin levels. Here, we developed an *HBB* gene replacement strategy using CRISPR-Cas9 that successfully addresses these challenges. We determined that a DNA donor containing a diverged *HBB* coding sequence and heterologous introns to avoid sequence homology provides proper physiological expression. We identified a DNA donor that uses truncated *γ-globin* introns, results in 34% HDR, and rescues β-globin expression in *in vitro* models of SCD and β-thalassemia in hematopoietic stem and progenitor cells (HSPCs). Furthermore, while HDR allele frequency dropped *in vivo*, it was maintained at ∼15%, demonstrating editing of long-term repopulating HSPCs. In summary, our *HBB* gene replacement strategy offers a differentiated approach by restoring naturally regulated adult hemoglobin expression.

INTRODUCTION

Hemoglobin is produced at high levels in red blood cells (RBCs), functioning to efficiently deliver oxygen to tissues throughout the body. The adult hemoglobin protein (HbA) is a tetramer consisting of two β-globin and two α-globin chains ($\alpha_2\beta_2$). Hemoglobinopathies are genetic disorders affecting either of the two globin chains. The two most common β-hemoglobinopathies are sickle cell disease (SCD) and β-thalassemia. SCD is caused by one point mutation (E6V) in the β-globin protein (β^S), which causes polymerization of hemoglobin-containing β^S chains, chronic hemolytic anemia, severe pain and other acute crises, progressive end-organ dysfunction, and early mortality.[1,2] In contrast, almost 300 different mutations spanning the *HBB* locus have been characterized for β-thalassemia. Individual mutations result either in the reduction or absence of β-globin, leading to an excess of non-functional, free α-globin chains.[3,4] A few medicines, such as hydroxyurea,[5] are available that provide symptom relief but no cure, and often show variable effectiveness in patients. Another small molecule, voxelotor,[6] showed effectiveness in the clinic but was recently withdrawn due to safety concerns. One available cure for both is an allogeneic hematopoietic stem cell transplant. However, the success of this treatment option is limited by low human leukocyte antigen (HLA)-matched donor availability and the complications of allograft rejection and graft-versus-host disease.[7] An alternate treatment approach is an autologous transplant paired with *ex vivo* fetal globin reactivation[8] or a lentiviral addition of a functional *HBB* gene,[9] which have recently been approved as therapies. However, while both autologous approaches appear to be effective, neither of them directly addresses the underlying cause of the disease: correcting and replacing the dysfunctional *HBB* gene.

We sought to develop an *ex vivo HBB* replacement strategy that maintains endogenous genetic control of the corrected *HBB* transgene to address most hemoglobinopathy genotypes. The genetic elements that transcriptionally activate β-globin are well studied and include an upstream enhancer called the locus control region (LCR), the β-globin promoter, β-globin introns, and 3′ regulatory regions.[10–12] We hypothesized that leveraging these *in situ* regulatory elements and replacing the dysfunctional *HBB* gene at its endogenous locus

Received 3 July 2024; accepted 25 February 2025;
https://doi.org/10.1016/j.ymthe.2025.02.036.

Correspondence: Matthew H. Porteus, Kamau Therapeutics, Inc., South San Francisco, CA 94080, USA.
E-mail: mporteus@kamautx.com
Correspondence: Beeke Wienert, Graphite Bio, Inc., South San Francisco, CA 94080, USA.
E-mail: b.wienert@outlook.com

should ensure efficient erythroid-specific transcription and physiological levels of β-globin. However, addressing all ≥300 mutations underlying SCD and β-thalassemia via a single *HBB* gene replacement requires a novel gene-editing strategy.

Successful insertion of larger gene cassettes using CRISPR-Cas9 and AAV6 donors can be achieved in hematopoietic stem and progenitor cells (HSPCs),[13–15] which led us to pursue *HBB* gene replacement by creating a double-strand break (DSB) in *HBB* exon 1 using CRISPR-Cas9[14] and replacing the whole gene by homology-directed repair (HDR) from the start codon onward. Two hurdles had to be overcome: (1) the replacement *HBB* gene cassette must contain the necessary genetic elements to promote physiological levels of *HBB* expression and (2) to avoid incomplete and unpredictable gene insertion outcomes, the DNA donor template must not be homologous to the endogenous *HBB* gene. By diverging the *HBB* coding sequence and using truncated heterologous *γ-globin* (*HBG2*) introns instead of β-*globin* introns, we achieved efficacious repair and potent β-globin expression in SCD HSPCs and β-globin knockout (KO; β-thalassemia-like) HSPCs. This work showcases a gene engineering approach that could correct most β-hemoglobinopathy genotypes.

RESULTS

The replaced *HBB* gene requires introns for physiological protein expression

Developing an *HBB* gene replacement cassette that is driven by the endogenous *in situ* promoter and LCR would conserve the regulatory elements of β-globin that are necessary for its physiological expression.[11,12,16] To accomplish this, one could excise the *HBB* gene with two single-guide RNAs (sgRNAs) and replace the *HBB* coding sequence.[17] However, each additional sgRNA raises the risk of unintended DSBs and inversions; consequently, our aim was to develop an *HBB* gene replacement strategy using a single sgRNA and HiFi-Cas9 targeting *HBB*.[14,18] We tested three different CRISPR-Cas9 approaches to knockin *HBB* coding sequences at the *HBB* locus: (1) gene replacement while maintaining the endogenous 3′ UTR polyadenylation sequence (pA) by using split homology arms, (2) gene insertion with a woodchuck hepatitis virus post-transcriptional response element (a genetic element known to increase the number of transcripts),[19] or (3) gene insertion with a bovine growth hormone pA tail (bGH-pA) (Figures S1A and S1B). To encourage HDR fidelity, we eliminated intronic sequences and diverged the WT *HBB* codons while maintaining the endogenous amino acid sequence (HBB^{div}) (Table S1). For screening readouts of HDR and resulting protein expression, we used a T2A-EGFP reporter system[15] (Figure S1C) measuring *HBB* transgene expression by EGFP mean fluorescence intensity (MFI) after 14 days of erythroid differentiation of edited HSPCs. As a positive control readout for physiological *HBB* expression, we also tagged the endogenous *HBB* gene with T2A-EGFP (Figure 1A). All three gene insertion strategies demonstrated that introducing the HBB^{div} coding sequence alone resulted in a >50% reduction in protein expression relative to wild type (WT), suggesting that introns might be necessary for physiological β-globin expression (Figure S1D).

Heterologous globin introns within the *HBB* gene cassette restore β-globin expression following HDR

We hypothesized that WT introns from alternative globin loci could function similarly because of the highly conserved exon-intron compositions across globin loci (three exons, two introns).[20] The conserved nature of their location within the coding sequence among vertebrates suggests similar splicing mechanisms.[21] We constructed four new HBB^{div} adeno-associated virus type 6 (AAV6) DNA donors containing full-length introns from either human or primate δ-globin (*HBD*i-hs or *HBD*i-pr, respectively), human γ-globin (*HBG2*i), or human α-globin (*HBA1*i) (Table S2). *HBA1* introns had the least sequence similarity and greatest difference in length, whereas the β-like *HBD* and *HBG2* introns aligned more closely to *HBB* (Figure 1B). We found that apart from *HBA1* introns, all heterologous introns restored HBB^{div}-T2A-EGFP expression to physiological levels (Figures 1C and S2A–S2D). To confirm that the T2A-EGFP flow-based readout reflected HBB expression, we removed T2A-EGFP and used high-performance liquid chromatography (HPLC) to measure hemoglobin. Since HBB^{div} hemoglobin is indistinguishable from unedited HBB, we incorporated the E6V SCD point mutation into the HBB^{div} (E6V-HBB^{div}) constructs and *HBB* gene (E6V-HBB; Figure S3A) as a control. To assess HDR frequencies of E6V-HBB^{div}, we developed a droplet digital PCR (ddPCR) method (Figures S3B and S3C). We determined HDR in HSPCs 2 days post-editing by ddPCR (E6V-HBB^{div}) or by amplicon next-generation sequencing (NGS) (E6V-HBB) and quantified hemoglobin S (HbS) tetramers over HbA and fetal hemoglobin (HbF) in erythroid progenitors. Building from our previous observations, although HDR frequencies were comparable, low HbS expression was found in samples with no introns (E6V-Δint), while high HbS expression was observed for E6V-HBB^{div} with heterologous introns and the E6V-HBB control (Figures 1D, S3D, and S3E). This finding confirmed that heterologous globin introns restore HBB^{div} expression to physiological levels and validated our T2A-EGFP reporter system results.

Truncating intron 2 maintains protein expression but reduces HBG2 recombination

Since the WT *HBG2* introns (HBG2i-WT) have the least homology to *HBB* introns and maintain protein expression, we engineered the HBB^{div}-HBG2i-WT AAV6 donor to improve expression or HDR frequencies. Globin mRNAs are unusually stable,[22–24] so we tested whether other globin UTRs or pA sequences (Table S3) could further boost expression. We saw no improvements in pA UTRs over bGH, concluding that the original bGH-pA construct was an efficient option (Figure S4A). Next, we attempted to truncate *HBG2* introns while maintaining protein expression by assembling 10 different AAV6 donors with deletions in one of the two introns or combinations thereof (Figure S4B; Table S4), while keeping splice sites and known branch points intact.[25–27] When tested in HSPC-derived erythroid progenitors, only the construct containing the HBG2i-i2v2 truncation, a deletion of 739 bp within intron 2, showed comparable protein expression levels to HBG2i-WT by EGFP MFI (Figure S4C) and was further investigated (Figure 2A).

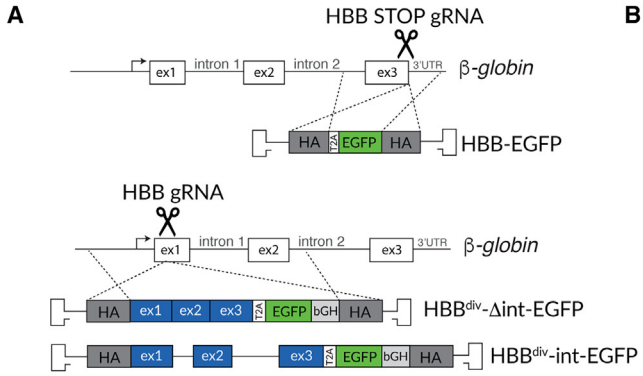

B

gene	intron length		homology to *HBB*	
	intron 1	intron 2	intron 1	intron 2
HBB	130bp	850bp	-	-
HBD (hs)	128bp	898bp	87.7%	48.4%
HBD (pr)	130bp	894bp	80.8%	47.4%
HBG2	122bp	886bp	52.0%	47.6%
HBA1	117bp	149bp	36.9%	14.3%

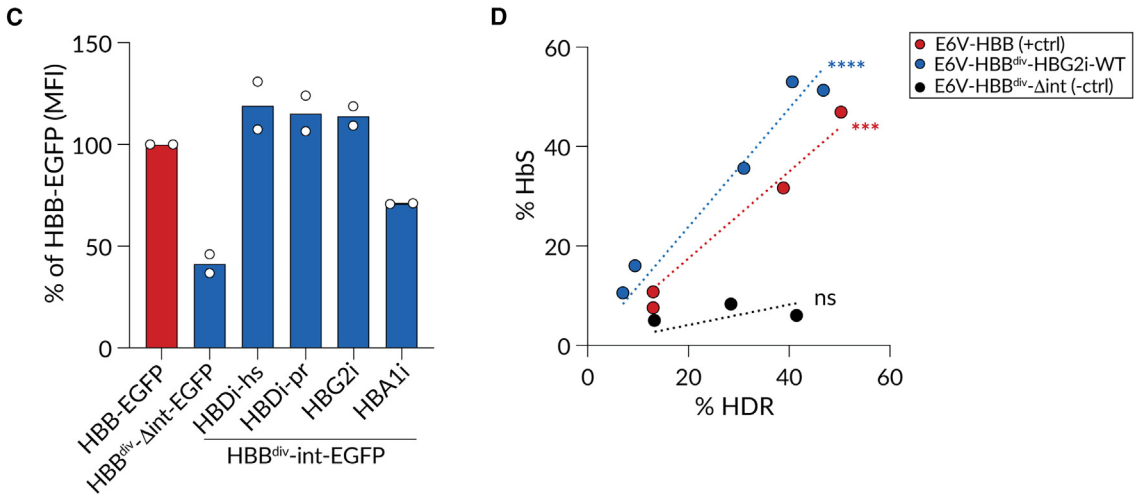

Figure 1. Heterologous globin introns rescue β-globin expression to physiological levels after gene replacement

(A) Schematic of two different gene-editing strategies at the *HBB* locus. Insertion of a T2A-EGFP sequence at the STOP codon of endogenous *HBB* (top, HBB-EGFP), and an *HBB* gene replacement cassette with diverged codons (HBB^{div}; see Figure S1B) containing either no introns (HBB^{div}-Δint-EGFP) or introns from different heterologous globin genes followed by a T2A-EGFP-bGH sequence (HBB^{div}-int-EGFP). (B) Table outlining the length and homology of globin introns tested relative to native *HBB* introns. (C) EGFP mean fluorescence intensity (MFI) of EGFP^{+} populations of *in vitro* differentiated erythroid progenitors edited with the AAV6 DNA donors outlined in (A). Shown is the MFI of EGFP^{+} cells normalized to the MFI for HBB-EGFP control for each experiment, $n = 2$. (D) HbS expression by HPLC and HDR allele frequency by ddPCR (E6V-HBB^{div}-HBG2i-WT and E6V-HBB^{div}-Δint) or amplicon NGS (E6V-HBB) of *in vitro* differentiated erythroid progenitors edited at the *HBB* locus to introduce the E6V SCD mutation (Figure S3A). The dotted line represents a linear regression for each construct. Statistical significance of experimentally determined slopes' difference to zero was calculated using a simple linear regression. Each data point represents a biological HSPC replicate. hs, *Homo sapiens*; ns, not significant; pr, primate. ***$p < 0.001$; ****$p < 0.0001$; bar graphs represent the mean.

We then evaluated potential differences between HBB^{div}-HBG2i-WT and truncated HBB^{div}-HBG2i-i2v2 donors in regard to HDR, hemoglobin expression, cell health, and gross genomic rearrangements (Figures 2A–2F). Despite the 739-bp truncation of HBB^{div}-HBG2i-i2v2, we found no differences between the two constructs in HDR, hemoglobin expression, or HSPC health (Figures 2B–2E and S4D). We also assessed the DNA damage response to our editing strategy by measuring p21 levels 24 h after gene editing (Figure S4E). While we observed an increase in p21 levels over untreated cells, no difference was observed between HBB^{div}-HBG2i-WT and HBB^{div}-HBG2i-i2v2. In addition, we did not observe a correlation between p21 signal and ability to form colony-forming units (CFUs) (Figure S4F). However, as nuclease independent site-specific homologous recombination has been reported in AAV applications,[28,29] we decided to survey genomic regions with the highest likelihood of gross genomic rearrangements with *HBB*. To survey the adjacent genomic landscape for potential gene editing effects, we implemented an amplification-free, multiplexed PacBio long-range sequencing (NoAmp PacBio) workflow[30] that can capture recombination events between the *HBG* and *HBB* genes and other structural variants (SVs, defined as >35-bp indels) without PCR amplicon size bias (Figures S5A and S5B). We sequenced DNA from edited HSPCs (Figures 2F, S5C, and S5D) and found that in HDR samples, correct in-frame HDR made up the majority of SV reads (25%–30%). Larger indels of 35–500 bp were found to a similar extent in ribonucleoprotein (RNP)-only and HDR samples (2%–5%). Detected inverted terminal repeat

(ITR) insertions were within reported norms of up to 7% of reads for cellular AAV delivery at 1.9% and 5.3% for HBB^{div}-HBG2i-WT and HBB^{div}-HBG2i-i2v2, respectively.[31–33] Interestingly, we discovered a recombination event between the *HBB* gene and the *HBG2* gene in one of the samples edited with HBB^{div}-HBG2i-WT, but not with the HBB^{div}-HBG2i-i2v2 (Figures 2F and S5C). No recombination events with the *HBG1* gene were observed in either sample type. As NoAmp PacBio is not strictly quantitative due to low read depth (Figures S5C and S5D), to probe for distinct recombination events, we designed a targeted ddPCR assay for the HBG-HBB recombination. Indeed, this orthogonal method identified that the HBB^{div}-HBG2i-i2v2 donor significantly reduced undesired recombination events between HBG and HBB compared to the HBB^{div}-HBG2i-WT donor (0.2% vs. 1.7%, respectively) (Figures 2F, S5E, and S5F). We engineered a compact DNA donor that sustains high protein expression, and by truncating intron 2 significantly reduced off-target HBG-HBB recombination.

HBB^{div}-HBG2i-i2v2 gene replacement rescues HbA expression in β-hemoglobinopathy models

Next, we investigated whether this approach could be used to rescue β-hemoglobinopathy genotypes *in vitro*. Two SCD patient HSPCs (SS genotypes) were edited and then differentiated for downstream readouts (Figure 3A). To compare HBB^{div}-HBG2i-i2v2 gene replacement to gene correction,[14,34] we also included a single-nucleotide polymorphism (SNP) donor, which corrects only a short stretch of *HBB* surrounding the E6V mutation.[14] Edited HSPCs maintained erythroid lineage differentiation potential (Figures S6A and S6B), and HDR frequencies averaged 50.3% for gene correction and 36.2% for gene replacement (Figure 3B). This is an expected difference due to the size of the insert[35] but remains consistent with previous WT HSPC HDR frequencies (Figure 2B). We compared hemoglobin expression by HPLC and reverse phase-HPLC (RP-HPLC) and found that both approaches rescued bulk HbA expression to levels seen in healthy SCD trait individuals, corresponding to more than 50% of total hemoglobin tetramers and a β:α globin chain ratio of >0.5 (Figures 3C and S7A–S7C). While elevated HbF levels upon β-globin KO[36] are commonly seen, we also observed that RNP-only samples produced small amounts of HbA. This is possibly due to small amounts of homologous repair guided by the endogenous *HBD* gene resulting in a functional *HBB* gene. Next, to ensure that splicing integrity was maintained in HBB^{div}-HBG2i-i2v2 mRNA, we performed bulk RNA sequencing (RNA-seq) on SCD erythroid progenitors. When *HBB* transcripts were mapped to *HBB* exons, no intronic differences were observed in the gene-edited samples compared to untreated samples. We concluded there was no abnormal intron retention or exon skipping as HBB^{div} reads were maintained across all three exons in HBB^{div}-HBG2i-i2v2 samples (Figure 3D). These data show that our gene replacement strategy can correct HbA expression in SCD HSPC-derived erythroid progenitors at protein and mRNA levels.

To create "β-thalassemia-like" HSPCs we knocked out *HBB* with two different RNPs targeting *HBB* exon 3 (*HBB* KO) in bulk WT HSPCs[37] (Figures 3E, S7D, and S7E). We chose exon 3 for the KO to avoid exon 1, which is necessary for the second step of gene replacement using HBB^{div}-HBG2i-i2v2. We then rescued bulk *HBB* KO cells with our HBB^{div}-HBG2i-i2v2 replacement and compared production of β-globin to parental *HBB* KO cells edited with RNP alone. As a control to account for stress-induced fetal globin induction, we also double-electroporated cells with non-targeting RNP (scramble, no known human target). Differentiated RNP-only *HBB* KO cells had near-undetectable levels of β-globin chains as measured by RP-HPLC, while β-globin expression was recovered to 45.2% of scramble (β:α-globin chain ratio of 0.4:1) once rescued with HBB^{div}-HBG2i-i2v2, with HDR frequencies of 22.2% (Figures 3F, 3G, S7D, and S7E). These experiments demonstrate that HBB^{div}-HBG2i-i2v2 gene replacement can restore *HBB* expression to trait levels in a β-thalassemia-like HSPC model.

HBB^{div}-HBG2i-i2v2 HDR-edited HSPCs engraft long term in immunodeficient mice

Next, we determined whether the HBB^{div}-HBG2i-i2v2 gene replacement is durable in long-term repopulating stem cells and whether these gene-edited HSPCs can reconstitute myeloid and lymphoid lineages *in vivo* (Figure 4A). WT HSPCs from two different donors were edited with RNP-only or HBB^{div}-HBG2i-i2v2 and cell viability, editing outcomes, CFU potential, and immunophenotypes measured (Figures S8A–S8G). Cell viability and HDR were consistent with prior observations with no discernible differences between RNP-only and HBB^{div}-HBG2i-i2v2 HSPCs (Figures S8A and S8B). All edited HSPCs were able to give rise to all multipotent lineages, although the editing process with AAV6 reduced the total number of colonies by ∼2-fold (Figure S8C). Additionally, the number of CFU-granulocyte, erythrocyte, monocyte, and macrophage colonies formed was lower in samples that underwent gene editing relative to unedited controls (Figure S8D). Although not statistically significant, this result was an anticipated outcome that is consistent with other reports.[37] Cells were characterized using an antibody panel defining a hematopoietic stem cell (HSC)-enriched population (CD34^{+}/CD45RA^{-}/CD90^{+}/CD38^{-})[38] (Figures S8E and S8F) and additional cell surface markers identifying long-term HSCs in culture (CD49c,[39] CD49f,[40,41] CD112,[42] CD201[43]) (Figure S8G). We found no significant difference in cell population frequencies between RNP-only and HBB^{div}-HBG2i-i2v2 cells, but we did find that gene editing decreased the frequency of the HSC-enriched and CD49f^{+} population compared to untreated cells cultured for the same amount of time (Figure S8G). The remaining edited HSPCs were injected into irradiated immunodeficient NSG mice. Sixteen weeks post-transplantation, bone marrow was harvested, and engraftment of human cells was assessed by human CD45 and HLA-A/B/C markers (Figures 4B and S9A). All groups successfully engrafted into the bone marrow with human chimerism ranging between 13% and 72% (Figure 4B). As previously described,[14,15,44–47] engraftment was negatively impacted by AAV6 transduction, but interestingly, the magnitude of the impact drastically differed between HSPC donors (Figure 4B). However, AAV6 transduction had no discernible impact on distribution of myeloid and lymphoid lineages *in vivo* (Figures 4C, S9B, and S9C). Finally, we determined HDR in the bulk population of

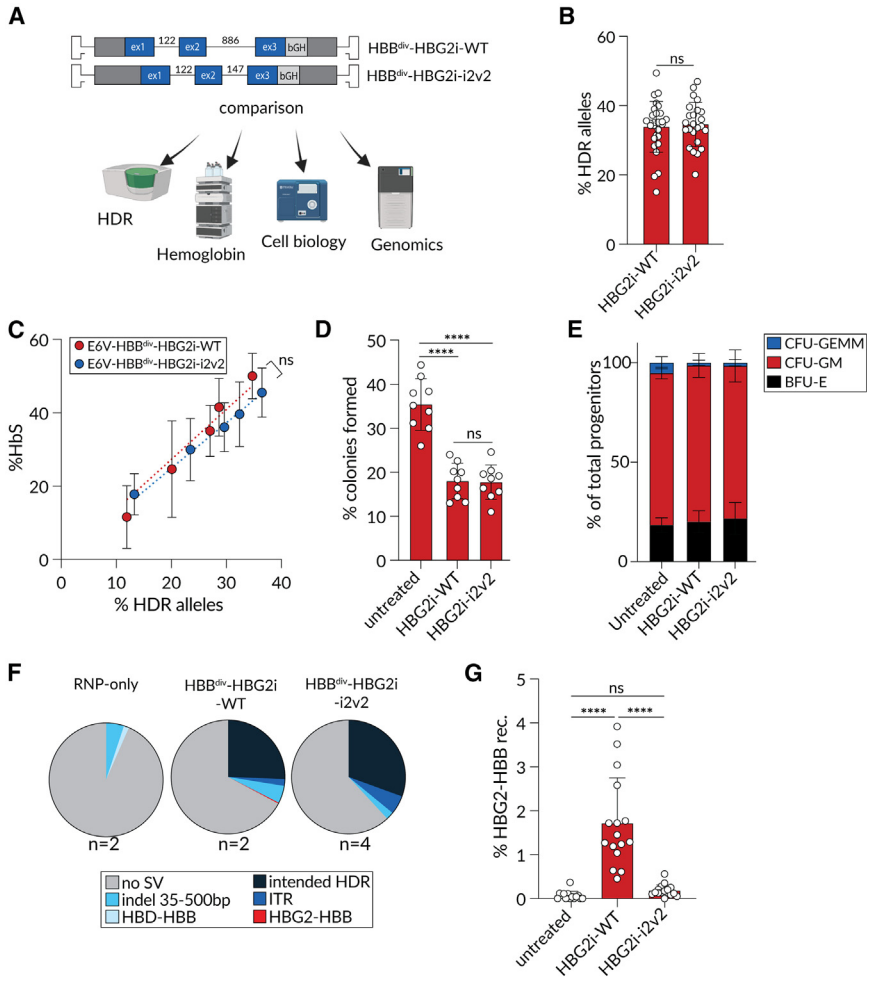

Figure 2. Truncating *HBG2* intron 2 maintains protein expression and reduces off-target recombination

(A) Schematic outlining the HBB^{div}-HBG2i-WT and the truncated (HBB^{div}-HBG2i-i2v2) AAV6 DNA donors and the assays used to compare their performance. (B) HDR frequencies in HSPCs edited with HBB^{div}-HBG2i-WT or HBB^{div}-HBG2i-i2v2 AAV6 donors determined by ddPCR (3′ assay; Figure S3B). Statistical significance was determined by unpaired two-tailed t test. n = 25 and 29 HSPC biological replicates, respectively. (C) HbS production by HPLC and HDR allele frequency by ddPCR (3′ assay) in HSPC-derived erythroid progenitors edited with E6V-HBB^{div}-HBG2i-WT or E6V-HBB^{div}-HBG2i-i2v2 AAV6 donors (n = 5 HSPC donors for each data point). Statistical significance was determined by first performing a non-linear regression for each construct. The analysis determined that the relationship between %HDR and %HbS was linear for each construct and is represented by the dotted lines. Next, the slopes were defined, and statistical significance was determined by an unpaired two-tailed t test comparing the slopes of the regression. (D) CFU frequency from *in vitro* cultured HSPCs edited with HBB^{div}-HBG2i-WT or HBB^{div}-HBG2i-i2v2 AAV6 donors. Shown is the percentage of colonies out of the total HSPCs plated. Statistical significance was determined by ordinary one-way ANOVA using Šídák's multiple comparisons test. (E) Distribution of lineages formed by colonies shown in (D) normalized to the total number of colonies formed (D and E) n = 9 HSPC replicates for all sample types, and each data point represents a biological replicate. (F) Frequency and types of events identified by PacBio NoAmp sequencing of HSPCs edited with RNP-only, HBB^{div}-HBG2i-WT, or HBB^{div}-HBG2i-i2v2 AAV6 donors, respectively. Structural variant (SV) analysis workflow (Figure S5B) classifies indels <35 bp and unedited reads as no SV. n = 2–4 HSPC donors. (G) ddPCR outcomes quantifying recombination events between *HBG* and *HBB* genes in HSPCs edited with HBB^{div}-HBG2i-WT or HBB^{div}-HBG2i-i2v2 AAV6 donors, respectively (HBG2-HBB assay). Cells were cultured according to the method for culture and gene editing of CD34$^+$ HSPCs. n = 16 biological replicates; statistical significance was determined by ordinary one-way ANOVA using Šídák's multiple comparisons test. ns, not significant; $^*p < 0.05$; $^{**}p < 0.01$; $^{****}p < 0.0001$; bar graphs represent the mean and the error bars represent standard deviation.

engrafted human HSPCs and found that HBB^{div}-HBG2i-i2v2 groups showed an average of 15.9% HDR, which equates to minimally 15.9% (if all homozygous) and maximally 31.8% (if all heterozygous) trait-genotype cells, with no significant differences between HSPC donors (Figure 4D). The fraction of HDR cells after engraftment was 2-fold lower than pre-engraftment, while non-homologous end joining (NHEJ) cells were 2-fold more persistent (Figures 4E and S10A), an observation that has previously been described[13–15,34] and may allude to the NHEJ pathway being predominant in long-term populating HSPCs.[41] Recombination events between *HBG* and *HBB* were 0.57% on average pre-engraftment and dropped to undetectable levels post-engraftment (Figure S10B). Then, we mapped allelic diversity based on amplicon NGS data to investigate clonality.[48] Annotating unique NHEJ events revealed a drop in allelic diversity post-engraftment (from ∼390 to 57–130 unique NHEJ events; Figures 4F and S10C), a reduction that is commonly seen in xenotransplantation studies tracking clonality.[48–51] In addition, we observed a significant decrease in diversity in HBB^{div}-HBG2i-i2v2 HSPCs compared to RNP-only (Figure 4F), further suggesting that AAV6 transduction may impact HSPC clonality *in vivo*.[45,50,51]

DISCUSSION

Here, we describe the development of an alternative *HBB* gene replacement approach that addresses three critical aspects required to treat β-hemoglobinopathies: first, it allows the *HBB* gene to be transcribed from its *in situ* endogenous locus, thereby maximizing expression of the repaired *HBB* gene; second, it replaces the full *HBB* gene from the start codon onward; and third, it restores HbA to physiological levels. Therefore, this gene replacement strategy includes the components necessary to correct the various *HBB* genotypes that give rise to SCD, SCD/β-thalassemia, and severe β-thalassemia (β^0). To further improve the safety of our approach, the donor

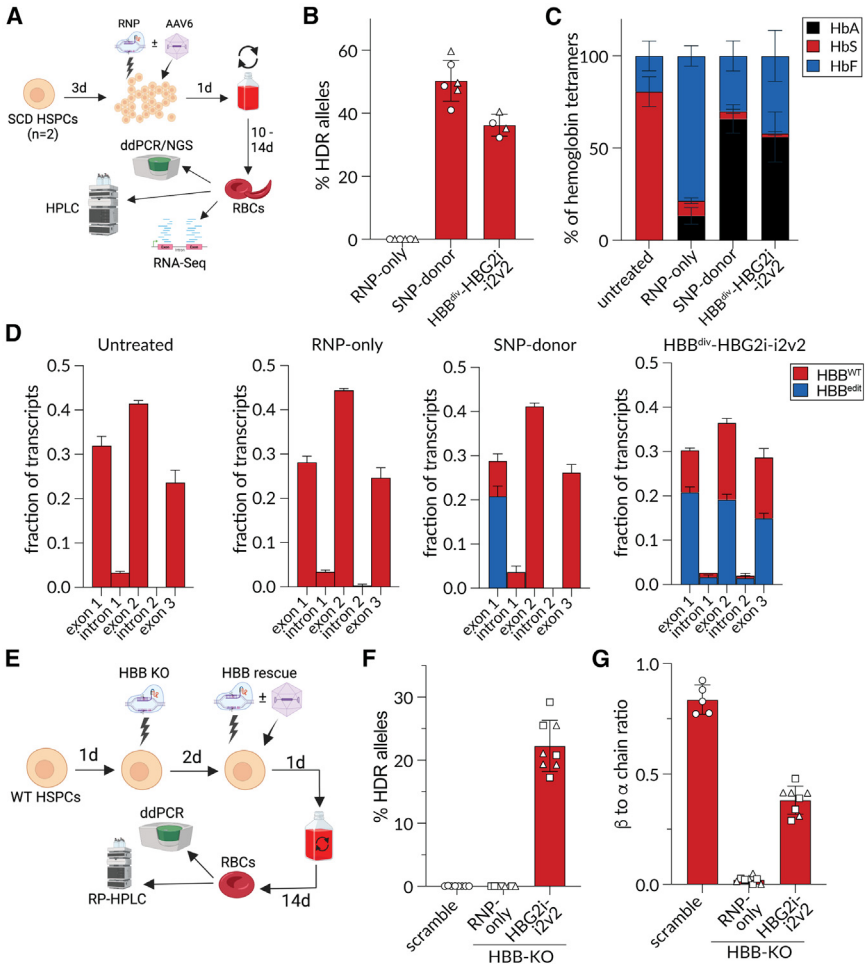

Figure 3. HBB gene replacement rescues disease phenotypes *in vitro*

(A) Schematic of the gene editing workflow for SCD HSPC *HBB* gene replacement. (B) HDR allele frequencies measured by amplicon NGS (SNP donor) or ddPCR (HBB^{div}-HBG2i-i2v2, 3′ assay). Each data point represents a biological replicate, and the shape (circle or triangle) indicates different SCD HSPC donors as follows: n = 6 for RNP-only and SNP donor or n = 4 for HBB^{div}-HBG2i-i2v2 biological replicates in two SCD HSPC donors. (C) Hemoglobin tetramer composition of SCD and gene-corrected SCD erythroid progenitors (day 14 of differentiation) measured by HPLC. Shown is the area for HbS, HbA, and HbF as a fraction of total area. Biological replicates were measured as n = 8 each for untreated, RNP-only, and SNP donor or n = 6 for HBB^{div}-HBG2i-i2v2 in two SCD HSPC donors. (D) Exon and intron transcript read coverage by RNA-seq of *in vitro* differentiated SCD erythroid progenitors (day 10). Shown is the fraction of *HBB* transcripts that contained sequences from each exon or intron, and within those, the fraction of transcripts that were gene edited (HBB^{Edit}). For SNP donor only exon 1 contains notable sequence differences after gene editing. Shown are data for n = 6 biological replicates in two SCD HSPC donors for each sample type. (E) Schematic overview of gene-editing workflow to rescue *HBB* KO (β-thalassemia-like) in bulk HSPCs. (F) HDR frequencies of edited HSPCs by ddPCR (HBB^{div}-HBG2i-i2v2, 3′ assay) (G) RP-HPLC ratios of β-globin to α-globin chains in gene-edited HSPC-derived erythroid progenitors. (F and G) Each data point represents a biological replicate, n = 8 for all groups in four healthy HSPC donors. Different shapes represent different HBB KO sgRNAs (circle = scramble, square = KO-HBB sgRNA 1, triangle = KO-HBB sgRNA 2). KO, knockout; RP-HPLC, reverse-phase HPLC. Bar graphs represent the mean and the error bars represent standard deviation.

template was engineered to include heterologous *HBG2* introns with little homology to the endogenous *HBB* introns, which ensures that physiological expression of β-globin is maintained (Figure 2C) and eliminates incomplete HDR (Figures 2F and S5C). In addition, significantly truncating the second intron reduced off-target recombination with endogenous *HBG2* to undetectable levels (Figure 2G), generating a compact DNA donor with an improved safety profile.

Multiple groups have published approaches to address β-globinopathies by gene repair.[14,15,52–55] Compared to existing approaches of fetal hemoglobin induction via *BCL11A*[56] repression[52,54] or gene modification by base editing,[57] our approach offers the potential advantage of restoring adult HbA expression. Our targeted gene editing approach also overcomes the risks of semi-random gene integration associated with lentiviral gene therapy.[53] While base and prime editors could circumvent the requirement for a homologous donor template and have shown success in several hemoglobinopathy contexts,[55,57–59] their use would require a different editing strategy for each β-thalassemia mutation. In contrast, our data demonstrate the ability to correct the majority of pathogenic genetic mutations in *HBB* by replacing the entire coding sequence spanning the 3′ end of exon 1 to the 5′ end of exon 3, which includes the 6-nt correction for SCD in exon 1 previously published.[14] In addition, this approach directly addresses the mutations causing hemoglobinopathies in the *HBB* gene itself rather than using a biologic workaround to upregulate fetal globin to compensate for the biology of the *HBB* mutations. Furthermore, our approach inserts an intron-modified *HBB* gene into the endogenous *HBB* locus, whereas Cromer et al.[15] inserted the *HBB* gene into the *HBA1* locus. Comparing the two strategies, we believe that our approach is advantageous because the corrective insert maintains regulation from its endogenous locus.

Intronic regulation is a long-studied, complicated topic. Previous studies found that *HBB* introns are necessary for high expression,[12] potentially due to enhancer elements within intron 2. Our finding that heterologous globin introns can be used in place of *HBB* introns and maintain high expression via endogenous regulation interestingly suggests that while both introns are required, their functionality seems to be sequence independent. We found that using *HBG2* introns, which only share 47%–52% sequence homology, was sufficient to

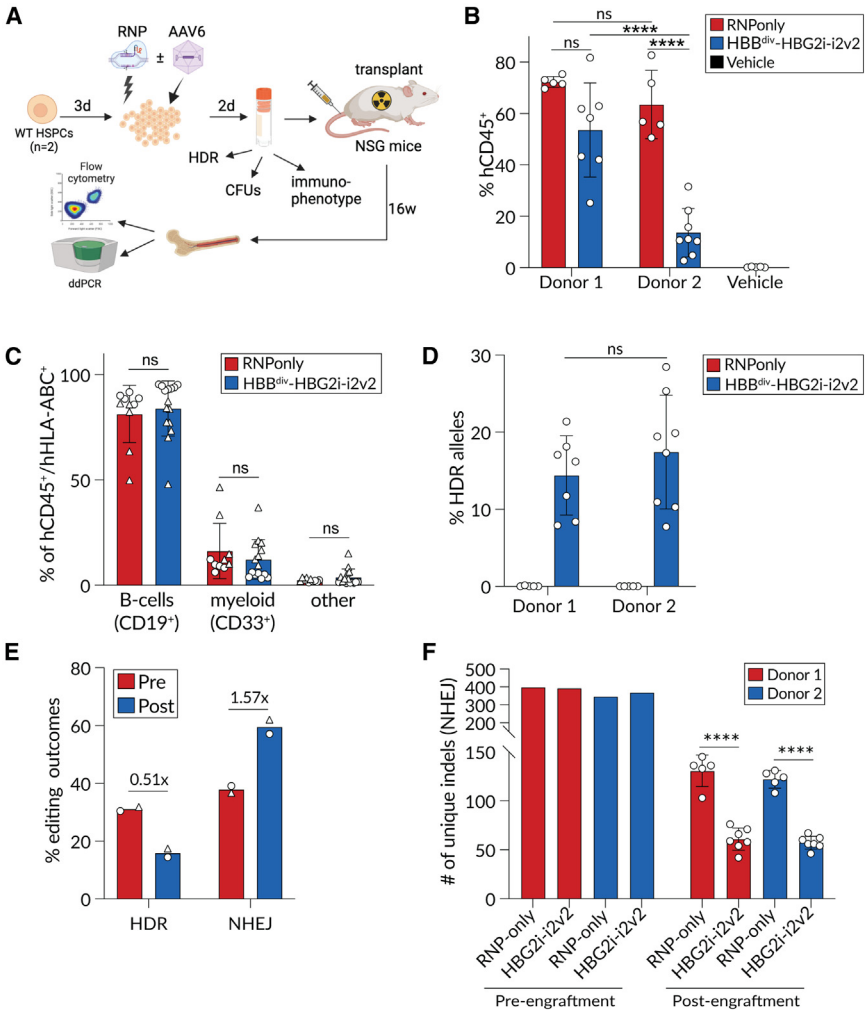

Figure 4. HBB^{div}-HBG2i-i2v2 alleles are retained after HSPC engraftment into immunodeficient mice

(A) Schematic of the transplantation experiment workflow. (B) At 16 weeks post-transplantation, mouse bone marrow was analyzed for human cell chimerism (%hCD45$^+$ as percentage of live) by flow cytometry. Gating strategy in Figure S9A. (C) Multilineage engraftment of human B (CD19$^+$) and myeloid (CD33$^+$) cells. Other cell types are further analyzed in Figures S9B and S9C. Circles = HSPC donor 1; triangles = HSPC donor 2. (D) HDR allele frequencies by ddPCR (3′ assay) in bulk hCD45$^+$ cells from bone marrow 16 weeks after transplant. (E) Comparison of editing outcomes in HSPCs pre- and post-engraftment. HDR was determined by ddPCR (3′ assay), and NHEJ was obtained by amplicon NGS. For post-engraftment samples the average of all mice within the respective group is shown. Donor 1, circles; donor 2, triangles. (F) Number of unique indel (NHEJ) events observed in samples pre-engraftment and in engrafted cells in each mouse represented in >0.001% of reads. (B–D and F) Statistical significance was calculated using a two-way ANOVA and Šídák's multiple comparisons test; ****$p < 0.0001$; error bars represent standard deviation. Each data point represents data from one mouse, unless otherwise noted. ns, not significant; bar graphs represent the mean and error bars represent standard deviation.

maintain physiological expression (Figures 1C and 1D). Similarly, using *HBD* introns from either human or primates resulted in the same outcome, suggesting that splicing of the mRNA to either increase stability or nuclear export[60] rather than *HBB* intron-specific regulatory elements is more important. Additionally, we observed that *HBA1* introns did not rescue expression to the same extent as β-like introns (*HBD*i and *HBG2*i; Figures S3D and S3E), which might indicate that there are inherent differences between β- and α-like globins, resulting in different regulation patterns. Initially, we hypothesized that intron function is size dependent because the second intron of *HBA1* is notably shorter than β-like globin introns (149 bp vs. ∼880 bp). However, since the truncated HBG2i-i2v2 (147 bp) maintained its functionality, we hypothesize that the integrity of specific branch points is more important than overall intron length.[27] Future studies to detail which globin intron structure and sequence influence protein expression may provide additional insight into globin gene regulation.

Our NoAmp PacBio long-range sequencing revealed interesting findings about SVs. In contrast to others,[61–63] we found no deletions greater than 500 bp within 10 kb of the cut site, except for a ∼6.7-kb deletion between *HBD* and *HBB* in RNP-only samples. We interpret this deletion as a recombination event between the highly homologous genes (Figure 2F). Using a multiplexed approach, we were also able to detect recombination events between the *HBG* and *HBB* genes, which are more than 27 kb apart. To the best of our knowledge, this is the first time a multiplexed NoAmp approach has been implemented to identify recombination events between two genomic loci. We propose that a similar multiplexed NoAmp approach could be used in other contexts to identify unknown SVs. Secondary validation methods are necessary, however, until an improved read depth allows for reliable quantification directly from the NoAmp sequencing datasets. The characterization of homologous off-target recombination in this study demonstrates that careful HDR template design is a necessary step in gene editing technology development.

Finally, while all groups of edited HSPCs successfully engrafted in xenotransplantation studies, our experiments revealed large donor-to-donor variability in chimerism of the mice injected with HBB^{div}-HBG2i-i2v2-edited HSPCs (Figure 4B) and a reduction in HDR (Figure 4E). This and recent data from Graphite Bio's nula-cel clinical trial[64–66] showing that HDR in engrafted HSCs is lower than anticipated when using a similar manufacturing approach, indicate that more work on improving the *ex vivo* gene editing process must be

done to make HDR a viable therapeutic strategy. Despite subjecting our edited HSPCs to widely accepted *in vitro* analysis, we were unable to predict this stark difference prior to engraftment. While CFU assay results generally predicted a reduction in engraftment by AAV6-transduced HSPCs, differences between the two donors were indistinguishable (Figures S8C and S8D) by this assay. Since RNP-only controls engrafted similarly between the two donors, the engraftment discrepancy observed cannot be inherent to the cell source but rather suggests that HSPCs from different donors react differently to AAV6 exposure and the DNA damage response it triggers. Given this result, to make our gene replacement a viable therapeutic strategy, AAV-mediated toxicity in the limited number of true HSCs needs to be overcome to improve engraftment outcomes and maintain polyclonality of the graft. For example, our team and others have previously shown that it is possible to lower the AAV6 dose by using a 53BP1 inhibitor to boost HDR without notable genotoxicity[67,68] while reducing the DNA damage response.[67] However, others observed that inhibiting DNA-dependent protein kinase results in gross genomic alterations,[67,69] highlighting the importance of continuing the careful interrogation of approaches that increase HDR. In addition, work published by several other groups identified transient P53 inhibition by various methods as an approach to markedly improve cell health. A brief delay in the P53 DNA damage response has been shown to reroute AAV-induced DNA damage, allowing time for cellular repair, rather than apoptosis induction or error prone repair.[45,46,49] However, safe levels and methods of P53 inhibition need to be carefully developed to ensure that P53 signaling is intact post-inhibition.[70] Furthermore, other groups have shown that choosing different HDR templates such as integrase-defective lentiviral vectors can reduce the DNA damage response and potentially improve engraftment success and clonality.[46] With the data presented here, we aim to disseminate observations that require careful evaluation and tracking in the hope to help the field address the many layers of cell health and behavior that affect HSPC engraftment potential. A recent study has shown that cellular responses and engraftment may vary in disease HSPCs compared to healthy donor cells.[71] Therefore, future work to validate our findings in β-thalassemia patient cells will be informative. Other future work will include improvements in the HSPC manufacturing workflows to ensure the maintenance of stemness and cellular health upon gene editing and establishing *in vitro* assays to better predict engraftment outcomes *in vivo*.[45,46,49,72]

In summary, our study lays the foundation for a differentiated *HBB* gene replacement strategy suitable for many β-hemoglobinopathy genotypes, including β^0/β^0, β^0/S, and hemoglobin C alleles.[73] The concept of using truncated heterologous *HBG2* introns we presented here also suggests that such an approach could be used in other contexts to boost transgene expression, guiding researchers to better genome engineering solutions.

MATERIALS AND METHODS

AAV production

AAV6 vectors were cloned into the pAAV-MCS plasmid (Agilent Technologies), containing ITRs from AAV2. AAV6 was produced in-house using 293FT cells (Thermo Fisher) or purchased as research-grade material from WuXi AppTec. Left and right homology arms (LHAs/RHAs) were PCRed from human genomic DNA to match the indicated length at the respective knockin sites. The diverged coding sequences including the introns were synthesized as gene fragments (Twist Bioscience or Genewiz) and cloned into pAAV with LHA and RHA via Gibson assembly (New England Biolabs). The 293FT cells (Thermo Fisher) were seeded in Millicell HY multilayer flasks (EMD) with $\sim 12.5 \times 10^7$ cells per flask. At 24 h later, each dish was transfected with a standard polyethylenimine transfection of 60 μg ITR containing plasmid and 220 μg pDP6 (Plasmid Factory GmbH), which contains the AAV6 cap genes, AAV2 rep genes, and Ad5 helper genes. After a 48- to 72-h incubation, cells were harvested and AAV purified using an AAVPro Purification Kit (All Serotypes) (Takara Bio USA) to extract full AAV6 capsids per the manufacturer's instructions. AAV6 vectors were then titered using ddPCR to measure the number of vector genomes and calculate vector genomes per cell.

Genome editing reagents and RNP formulation

sgRNAs were purchased with 2′-*O*-methyl-3′-phosphorothioate modifications (Synthego). Protospacers are listed in Table S5. High-fidelity Cas9 protein (SpyFi Cas9) was purchased from Aldevron. RNPs were complexed at a Cas9:sgRNA molar ratio of 1:2.5 at 25°C for 10–15 min prior to electroporation.

Culture and gene editing of CD34$^+$ HSPCs

Healthy donor human CD34$^+$ HSPCs were purchased from AllCells and isolated from Plerixafor and granulocyte-colony-stimulating factor-mobilized peripheral blood. SCD patient-derived HSPCs (homozygous for the E6V mutation) were obtained through Dr. John Tisdale (NIH) in compliance with Health Insurance Portability and Accountability Act regulations. HSPCs were cultured at 2.5×10^5–5×10^5 cells/mL in GMP SCGM (CellGenix) supplemented with stem cell factor (SCF), thrombopoietin, FLT3-ligand, interleukin-6 (100 ng/mL each; Peprotech), and UM171[74] (35 nM; SelleckChem). HSPCs were cultured at 37°C, 5% CO_2, 5% O_2 for 72 h. Next, cells were mixed with MaxCyte electroporation buffer and RNP (Table S5) and electroporated (MaxCyte; HSC-6), recovered 10 min at 37°C before plating at 3.5×10^5 cells/mL in cytokine-supplemented media containing AAV6 (2.5×10^3 vector genomes/cell). Cells were washed after 16–24 h to remove AAV6.

In vitro differentiation and immunophenotyping of erythroid progenitors

At 18–24 h post-electroporation, HSPCs were resuspended at 5×10^4–1×10^5 cells/mL in SFEMII medium with 1× Erythroid Expansion Supplement (both STEMCELL Technologies) (37°C, 5% CO_2) for 1 week before transfer to a secondary medium (SFEMII with SCF 10 ng/mL, erythropoietin 3 U/mL (both Peprotech), transferrin 200 μg/mL, and 3% human AB serum [Sigma-Aldrich]) at 1×10^5 cells/mL for 4 days. Cells were transferred to a terminal medium (SFEMII with erythropoietin 3 U/mL, transferrin 1 mg/mL, and 3% human AB serum) and maintained at 1×10^6 cells/mL for 4 days.

Differentiated cells were analyzed for CD34, CD45, CD71, and CD235a expression using antibodies listed in Table S6. Analysis was performed using FlowJo software.

Allelic targeting by ddPCR

Genomic DNA (gDNA) was enzymatically digested, and 12.5 ng/μL was added to the PCR reaction with Multiplex Supermix and primers/probes (Table S7). Droplet generation, PCR, and detection were performed according to the manufacturers' instructions (QX200 ddPCR System, Bio-Rad) to detect HDR (3′ assay or 5′ assay) or HBG2-HBB recombination.

Amplicon NGS for gene-editing outcomes

gDNA was amplified using primers (Table S8) and KAPA HiFi HotStart ReadyMix (Roche). A second PCR with primers containing Nextera sequencing adapters enriched the target locus. Individual samples were indexed using xGen UDI IDT index primers (IDT). Samples were pooled, sequenced on an Illumina Miseq, and analyzed as described below.

Analysis of amplicon NGS data

After demultiplexing, fastq files for each sample were analyzed with CRISPResso version 2.1.0. CRISPResso command-line arguments were "–amplicon_seq TCACTAGCAACCTCAAACAGACACCATGGTGCACCTGACTCCTGAGGAGAAGTCTGCCGTTACTGCCCTGTGGGGCAAGGTGAACGTGGATGAAGTTGGTGGTGAGGCCCTGGGCAGGTTGGTATCAAGGTTACAAGACAGG \

-e TCACTAGCAACCTCAAACAGACACCATGGTGCACCTGACTCCTGAGGAAAAATCCGCAGTCACTGCCCTGTGGGGCAAGGTGAACGTGGATGAAGTTGGTGGTGAGGCCCTGGGCAGGTTGGTATCAAGGTTACAAGACAGG \

–amplicon_name HBB_WT \

-g CTTGCCCCACAGGGCAGTAA \

–guide_name sgRNA_HBB \

–plot_window_size 50 \

-p 72 \

–skip_failed"

For analyzing indel clones, results from CRISPResso were post-processed using a custom Python script to extract the individual amplicons identified by CRISPResso. Each amplicon was labeled with a special string based on the specific modifications observed at the cutsite (insertions, substitutions, deletions). Amplicons with edits outside the cut site were assumed to be sequencing errors and collapsed into other amplicons.

Hemoglobin tetramer analysis by HPLC

A total of 4×10^5 erythroid progenitors were lysed in H_2O. Supernatant was cleared, diluted in buffer A, and analyzed using normal-phase ion exchange HPLC (PolyCAT A, 35 × 4.6 mm, 3 μm, 1,500 Å). Buffer A: 2 mM NaCN, 20 mM BisTris pH 6.9; buffer B: 2 mM NaCN, 200 mM NaCl, 20 mM BisTris pH 6.5. The maximum pressure (600 bar) and flow rates (1.5 mL/min) were consistent. Gradient ([min]/[%B]): 0/10%-8/40%-17/90%-20/10%-25/10%-stop.

Reverse-phase HPLC globin chain analysis

Hemoglobin lysates were prepared as described above and run on a 3.6-μM wide pore column (XB-C18 250 × 4.6 mm, Phenomenex Aeris) heated to 70°C. Buffer A: 6.4 mM NaOH, 0.1% trifluoroacetic acid (TFA), in water; buffer B: 1% TFA in acetonitrile. The maximum pressure was constant at 600 bar, while the flow rate was variable. Gradient ([min]/[%B]): 0/40%-1/41%-10/47% at 1 mL/min, 11/80%-16/20% at 0.5 mL/min, 17/40% at 1 mL/min, stop.

CFU progenitor assay

At 48 h post-editing, 250 cells/well were plated in Methocult Optimum media in 6-well SmartDish plates. The plates were incubated at 37°C, 5% CO_2, and 5% O_2 for 14 days before scoring colonies using the human mPB program on a STEMvision imager (all STEMCELL Technologies).

PacBio long-range sequencing library preparation

PacBio libraries were generated using the NoAmp protocol. High-molecular-weight (HMW) gDNA was extracted using 100G Genomic Tips (Qiagen) from 2 million cells 2 days post-editing. DNA purity and integrity was assessed with an Agilent 4200 TapeStation with Genomic DNA Screen Tape (Agilent). Three samples were multiplexed in a single library (6 mg HMW gDNA/sample). The 5′ and 3′ phosphates were removed from DNA with recombinant shrimp alkaline phosphatase (New England Biolabs) after incubating for 1 h at 37°C and 65°C for 15 min. The β-globin gene cluster was enriched by Cas9-RNP (New England Biolabs) digestion in two 10-kb fragments (γ-globin and β-globin fragments) at 37°C for 1 h. The sgRNA sequences used are listed in Table S5. Annealed PacBio SMRTbells were ligated to fragments with T4 DNA Ligase (Thermo Fisher Scientific) at 16°C for 2 h, and the enzyme heat inactivated at 65°C. Samples were pooled, and the libraries were cleaned with Exonuclease III (New England Biolabs) and the SMRTbell Enzyme Clean up kit (PacBio) for 2 h at 37°C and further cleaned with proteomics grade trypsin (VWR) for 20 min. Final libraries were sequenced on a PacBio Sequel IIe for 30 h. The resulting FASTQ files containing the reads were mapped to chromosome 11 (hg38 assembly) using default parameters with minimap2 (version 2.24). SVs were identified with Sniffles (version 1.0.7) using a cutoff of three or more supporting reads to identify an individual SV.

PacBio long-range sequencing

HMW gDNA was extracted and dephosphorylated. The β-globin gene cluster was enriched by Cas9-RNP digestion (Table S5). Libraries were finished via SMRTBell ligation and pooled and

sequenced on a PacBio Sequel. FASTQ files were used as input files to align to chromosome 11 (hg38) by minimap2 (version 2.24) using default parameters. The alignment BAM files were used to detect SVs (if they had >3 supporting reads) by Sniffles (version 1.0.7). "*sniffles -i mapped_input.bam -v output.vcf –minsupport 3*". Default criteria were used for remaining Sniffles parameters.

RNA-seq

Total RNA from day 10 erythroid progenitors was extracted. Sequencing libraries were generated using an Illumina TruSeq Stranded mRNA sample prep kit and sequenced on NovaSeq version 1.5 (both Illumina) using paired-end 2 × 150-bp reads by SeqMatic. Hypothetical post-editing reference genomes were created for each construct (hg38). RNA-seq reads were aligned with STAR (version 2.7.3a). Read counts for exons were computed with HTSeq count as outlined below. Exon/intron counts were normalized by length such that the total expression of the *HBB* gene (sum of WT and edited exon/intron expression) is 1—analogous to standard transcripts-per-million normalization for full-length transcripts but applied to individual exons/introns.

Parameters for HTSeq count of exon/intron analysis

The parameters used were as follows: Feature Type = Exon, ID attribute = exon_id, Mode = union, order = pos, stranded = no, additional_attr = exon_id, nonunique = all, secondary alignments = score. For intron read counts the following parameters were used: Feature Type = Intron, ID attribute = intron_id, Mode = union, order = pos, stranded = no, additional_attr = intron_id, nonunique = all, secondary alignments = score.

To quantify the allele fractions of exon 1 for the SNP donor, the RNA-seq reads were mapped to the reference (Hg38) using STAR (version 2.7) aligner (basic two-pass method) to produce a BAM file. Then, the frequencies of the five expected SNPs in exon 1 of *HBB* were extracted using igvtools (version 2.14.0) and averaged to estimate the WT and edited allele fractions.

Immunophenotyping of cultured HSPCs pre-engraftment

Edited HSPCs were washed and incubated with a panel of fluorochrome-conjugated anti-human monoclonal antibodies (mAbs; Table S6). Data were analyzed with CellEngine software.

HSPCs were washed with Cell Staining Buffer (CSB) (BioLegend). Cells were incubated with a panel of fluorochrome-conjugated anti-human mAbs and viability dye (Table S6). Brilliant Stain Buffer Plus (BD Bioscience) was added for stabilization. Cells were stained for 30 min at 4°C, washed with CSB, and acquired on a Fortessa X-20 (BD Biosciences) collecting 100,000–500,000 leukocyte events per sample. Fluorescence minus one (FMO) sample controls were prepared and acquired to facilitate gating. Ultracomp eBeads (Thermo Fisher) were stained with each fluorochrome-conjugated antibody, and heat-killed cells were stained with DyLight 800 Maleimide and used for software-based compensation. Data were analyzed with CellEngine software.

Immunophenotyping of engrafted human cells

At 16 weeks following transplantation of edited $CD34^+$ HSPCs, mice were euthanized, bones (2 femora, 2 tibiae, 1 pelvis) were collected and scraped, removing all muscle and fascia, and centrifuged to collect bone marrow. ACK lysing buffer (Gibco) was added, and cells were transferred to a 50-mL conical on ice for 5 min. Cells were washed with PBS+2% fetal bovine serum (FBS), resuspended in RPMI+2% FBS, filtered (70 μm strainer), and counted. Freshly isolated bone marrow mononuclear cells were washed, resuspended in CSB (BioLegend), and stained with a fluorochrome-conjugated mAb panel (Table S6). Brilliant Stain Buffer Plus (BD Bioscience) was added for stabilization. Cells were blocked with Human TruStain FcX (BioLegend) and Mouse TruStain FcX (BioLegend) for 10 min, then stained with the antibody cocktail for 30 min at 4°C. Cells were washed, filtered (70 μm), and acquired on a Fortessa X-20 (BD Biosciences) collecting 100,000–500,000 leukocyte events per sample. FMO controls were acquired to facilitate gating. Ultracomp eBeads compensation beads (Thermo Fisher Scientific) were individually stained with each fluorochrome-conjugated antibody, and ArC amine reactive compensation beads (Thermo Fisher Scientific) were stained with Fixable Viability Stain 780 and used for software-based compensation. Data were analyzed with FlowJo software version 10.8.1.

HSPC transplantation into immunodeficient NSG mice

Xenotransplantation studies were performed by Explora BioLabs with Institutional Animal Care and Use Committee approval. A total of 30 six-week-old female NSG mice were irradiated at 250 cGy. Three groups of mice (vehicle only, RNP-only, and HBB^{div}-HBG2i-i2v2) were injected with 5×10^6 viable $CD34^+$ HSPCs per mouse via tail vein. At 16 weeks following transplantation, mice were euthanized, bones were collected, RBCs were lysed, and cells were stained with a fluorochrome-conjugated antibody panel (Table S6). Data were analyzed with FlowJo software.

Analysis of NHEJ and HDR events in gene-edited HSPCs

Data from amplicon NGS (WT) and NHEJ and ddPCR (HDR) was combined. Using CRISPResso report files, unedited reads were labeled as "WT," whereas indels were grouped together as "NHEJ." These two groups were aggregated to %HDR from ddPCR and normalized to 100%. Genotype diversity was reported as the number of unique indel sequences with >0.001% total reads.

DATA AVAILABILITY

RNA-seq, PacBio, and NGS data are available at GEO under accession number GSE229212.

ACKNOWLEDGMENTS

We would like to thank Dr. John Tisdale and the National Institutes of Health for providing us with the SCD HSPCs. In addition, we would like to thank Dr. Euan Slorach and Dr. Rajiv Sharma for their guidance in the execution of the project and Dr. Josh Lehrer, Dr. Wes Miller, and Wayne Szeto for reviewing the manuscript. We would also like to acknowledge BioRender for schematics.

AUTHOR CONTRIBUTIONS

D.P.D., B.W., and K.A.W. conceived the study. B.W., A.R.C., K.A.W., and C.B. cloned and generated AAV6 donors. K.A.W., T.L.G., B.W., and C.B. cultured, edited, and differentiated HSPCs. T.L.G. and J.R.P. performed HPLC. K.A.W., B.W., T.L.G., and C.L.E. developed and ran the ddPCR. K.A.W., T.L.G., A.R.C., and B.J.Q. performed the CFU assays. C.D.L., K.A.H., W.M.M., and S.T. generated and analyzed the amplicon NGS data. C.D.L., C.L.E., K.A.W., B.W., and G.A. generated and analyzed the PacBio NoAmp data. K.A.W., B.W., W.M.M., K.K., and G.A. generated and analyzed the RNA-seq data. K.A.W., T.L.G., J.A.P.-B., Y.G.S., and B.J.Q. generated HSPCs for the xenotransplantation study. L.C., J.E.V., K.A.W., T.L.G., J.A.P.-B., B.J.Q., G.M.C., B.J.S., and T.D.K. processed the animal bones and generated data for the transplantation study. G.M.C., B.J.S., and T.D.K. performed the immunophenotyping of the HSPCs. B.W., D.P.D., S.K., and K.A.W. wrote the manuscript, with input from M.H.P., J.L.G., and all the other authors.

DECLARATION OF INTERESTS

All authors are former employees of Graphite Bio, Inc. and may own stock/options in the company, and all work was done while authors were employed at Graphite Bio, Inc.. A patent application encompassing aspects of this work has been filed, with C.B., A.R.C., D.P.D., and B.W. included as inventors and Graphite Bio, Inc. as the applicant (PCT/US2022/024477, pending). M.H.P. serves on the scientific advisory board of Allogene Tx and is an advisor to Versant Ventures; he has equity in CRISPR Tx and serves on the board of directors of Kamau Therapeutics; and he is affiliated with Stanford University. J.L.G. is an advisor to Kamau Therapeutics. K.A.W. and M.H.P. are current employees and shareholders of Kamau Therapeutics. B.W. is affiliated with and has equity in Evercrisp Biosciences. T.L.G. and L.C. are affiliated with Scribe Therapeutics. C.L.E. is affiliated with the University of California, San Francisco. J.A.P.-B. is affiliated with Genentech. J.R.P. is affiliated with Novartis. W.M.M. and A.R.C. are affiliated with Enceladus Biosciences. K.K. is affiliated with Bio-Rad Laboratories. S.K. is affiliated with and has equity in CRISPR Tx. C.D.L. is affiliated with OmniAb. G.M.C. is affiliated with Caribou Biosciences. J.E.V. is affiliated with Alector. B.J.S. is affiliated with Senti Biosciences. B.J.Q. is affiliated with the University of California, San Diego. K.A.H. is affiliated with Amber Biosciences. J.L.G. is affiliated with Biogen.

SUPPLEMENTAL INFORMATION

Supplemental information can be found online at https://doi.org/10.1016/j.ymthe.2025.02.036.

REFERENCES

1. Tisdale, J.F., Thein, S.L., and Eaton, W.A. (2020). Treating sickle cell anemia. Science *367*, 1198–1199.
2. Kato, G.J., Piel, F.B., Reid, C.D., Gaston, M.H., Ohene-Frempong, K., Krishnamurti, L., Smith, W.R., Panepinto, J.A., Weatherall, D.J., Costa, F.F., and Vichinsky, E.P. (2018). Sickle cell disease. Nat. Rev. Dis. Primers *4*, 18010.
3. Thein, S.L. (2013). The molecular basis of β-thalassemia. Cold Spring Harb. Perspect. Med. *3*, a011700.
4. Thein, S.L. (2005). Pathophysiology of beta thalassemia–a guide to molecular therapies. Am. Soc. Hematol. Educ. Program, 31–37.
5. Charache, S., Terrin, M.L., Moore, R.D., Dover, G.J., Barton, F.B., Eckert, S.V., McMahon, R.P., and Bonds, D.R. (1995). Effect of hydroxyurea on the frequency of painful crises in sickle cell anemia. N. Engl. J. Med. *332*, 1317–1322.
6. Vichinsky, E., Hoppe, C.C., Ataga, K.I., Ware, R.E., Nduba, V., El-Beshlawy, A., Hassab, H., Achebe, M.M., Alkindi, S., Brown, R.C., et al. (2019). A phase 3 randomized trial of voxelotor in sickle cell disease. N. Engl. J. Med. *381*, 509–519.
7. Fleischhauer, K., Locatelli, F., Zecca, M., Orofino, M.G., Giardini, C., De Stefano, P., Pession, A., Iannone, A.M., Carcassi, C., Zino, E., and La Nasa, G. (2006). Graft rejection after unrelated donor hematopoietic stem cell transplantation for thalassemia is associated with nonpermissive HLA-DPB1 disparity in host-versus-graft direction. Blood *107*, 2984–2992.
8. Frangoul, H., Locatelli, F., Sharma, A., Bhatia, M., Mapara, M., Molinari, L., Wall, D., Liem, R.I., Telfer, P., Shah, A.J., et al. (2024). Exagamglogene autotemcel for severe sickle cell disease. N. Engl. J. Med. *390*, 1649–1662.
9. Kanter, J., Walters, M.C., Krishnamurti, L., Mapara, M.Y., Kwiatkowski, J.L., Rifkin-Zenenberg, S., Aygun, B., Kasow, K.A., Pierciey, F.J., Bonner, M., et al. (2022). Biologic and clinical efficacy of lentiglobin for sickle cell disease. N. Engl. J. Med. *386*, 617–628.
10. Antoniou, M., Geraghty, F., Hurst, J., and Grosveld, F. (1998). Efficient 3'-end formation of human beta-globin mRNA in vivo requires sequences within the last intron but occurs independently of the splicing reaction. Nucleic Acids Res. *26*, 721–729.
11. Collis, P., Antoniou, M., and Grosveld, F. (1990). Definition of the minimal requirements within the human beta-globin gene and the dominant control region for high level expression. EMBO J. *9*, 233–240.
12. Morgan, R.A., Ma, F., Unti, M.J., Brown, D., Ayoub, P.G., Tam, C., Lathrop, L., Aleshe, B., Kurita, R., Nakamura, Y., et al. (2020). Creating New β-Globin-Expressing Lentiviral Vectors by High-Resolution Mapping of Locus Control Region Enhancer Sequences. Mol. Ther. Methods Clin. Dev. *17*, 999–1013.
13. Bak, R.O., Dever, D.P., and Porteus, M.H. (2018). CRISPR/Cas9 genome editing in human hematopoietic stem cells. Nat. Protoc. *13*, 358–376.
14. Dever, D.P., Bak, R.O., Reinisch, A., Camarena, J., Washington, G., Nicolas, C.E., Pavel-Dinu, M., Saxena, N., Wilkens, A.B., Mantri, S., et al. (2016). CRISPR/Cas9 β-globin gene targeting in human haematopoietic stem cells. Nature *539*, 384–389.
15. Cromer, M.K., Camarena, J., Martin, R.M., Lesch, B.J., Vakulskas, C.A., Bode, N.M., Kurgan, G., Collingwood, M.A., Rettig, G.R., Behlke, M.A., et al. (2021). Gene replacement of α-globin with β-globin restores hemoglobin balance in β-thalassemia-derived hematopoietic stem and progenitor cells. Nat. Med. *27*, 677–687.
16. Li, Q., Harju, S., and Peterson, K.R. (1999). Locus control regions: coming of age at a decade plus. Trends Genet. *15*, 403–408.
17. Cai, L., Bai, H., Mahairaki, V., Gao, Y., He, C., Wen, Y., Jin, Y.-C., Wang, Y., Pan, R.L., Qasba, A., et al. (2018). A Universal Approach to Correct Various HBB Gene Mutations in Human Stem Cells for Gene Therapy of Beta-Thalassemia and Sickle Cell Disease. Stem Cells Transl. Med. *7*, 87–97.
18. DeWitt, M.A., Magis, W., Bray, N.L., Wang, T., Berman, J.R., Urbinati, F., Heo, S.J., Mitros, T., Muñoz, D.P., Boffelli, D., et al. (2016). Selection-free genome editing of the sickle mutation in human adult hematopoietic stem/progenitor cells. Sci. Transl. Med. *8*, 360ra134.
19. Zufferey, R., Donello, J.E., Trono, D., and Hope, T.J. (1999). Woodchuck hepatitis virus posttranscriptional regulatory element enhances expression of transgenes delivered by retroviral vectors. J. Virol. *73*, 2886–2892.
20. Hardison, R.C. (2012). Evolution of hemoglobin and its genes. Cold Spring Harb. Perspect. Med. *2*, a011627.
21. Wieringa, B., Hofer, E., and Weissmann, C. (1984). A minimal intron length but no specific internal sequence is required for splicing the large rabbit beta-globin intron. Cell *37*, 915–925.
22. Weiss, I.M., and Liebhaber, S.A. (1995). Erythroid cell-specific mRNA stability elements in the alpha 2-globin 3' nontranslated region. Mol. Cell. Biol. *15*, 2457–2465.
23. Russell, J.E., and Liebhaber, S.A. (1996). The stability of human beta-globin mRNA is dependent on structural determinants positioned within its 3' untranslated region. Blood *87*, 5314–5323.
24. Peixeiro, I., Silva, A.L., and Romão, L. (2011). Control of human beta-globin mRNA stability and its impact on beta-thalassemia phenotype. Haematologica *96*, 905–913.
25. Will, C.L., and Lührmann, R. (2011). Spliceosome structure and function. Cold Spring Harb. Perspect. Biol. *3*, a003707.
26. Pineda, J.M.B., and Bradley, R.K. (2018). Most human introns are recognized via multiple and tissue-specific branchpoints. Genes Dev. *32*, 577–591.
27. Emery, D.W., Morrish, F., Li, Q., and Stamatoyannopoulos, G. (1999). Analysis of gamma-globin expression cassettes in retrovirus vectors. Hum. Gene Ther. *10*, 877–888.
28. Porteus, M.H., Cathomen, T., Weitzman, M.D., and Baltimore, D. (2003). Efficient gene targeting mediated by adeno-associated virus and DNA double-strand breaks. Mol. Cell. Biol. *23*, 3558–3565.
29. Russell, D.W., and Hirata, R.K. (1998). Human gene targeting by viral vectors. Nat. Genet. *18*, 325–330.
30. Tsai, Y.-C., Greenberg, D., Powell, J., Hoijer, I., Ameur, A., Strahl, M., Ellis, E., Jonasson, I., Mouro Pinto, R., Wheeler, V., et al. (2017). Amplification-free, CRISPR-Cas9 Targeted Enrichment and SMRT Sequencing of Repeat-Expansion

Disease Causative Genomic Regions. Preprint at bioRxiv. https://doi.org/10.1101/203919.

31. Gil-Farina, I., Fronza, R., Kaeppel, C., Lopez-Franco, E., Ferreira, V., D'Avola, D., Benito, A., Prieto, J., Petry, H., Gonzalez-Aseguinolaza, G., and Schmidt, M. (2016). Recombinant AAV integration is not associated with hepatic genotoxicity in nonhuman primates and patients. Mol. Ther. *24*, 1100–1105.

32. Nelson, C.E., Wu, Y., Gemberling, M.P., Oliver, M.L., Waller, M.A., Bohning, J.D., Robinson-Hamm, J.N., Bulaklak, K., Castellanos Rivera, R.M., Collier, J.H., et al. (2019). Long-term evaluation of AAV-CRISPR genome editing for Duchenne muscular dystrophy. Nat. Med. *25*, 427–432.

33. Miller, D.G., Petek, L.M., and Russell, D.W. (2004). Adeno-associated virus vectors integrate at chromosome breakage sites. Nat. Genet. *36*, 767–773.

34. Lattanzi, A., Camarena, J., Lahiri, P., Segal, H., Srifa, W., Vakulskas, C.A., Frock, R.L., Kenrick, J., Lee, C., Talbott, N., et al. (2021). Development of β-globin gene correction in human hematopoietic stem cells as a potential durable treatment for sickle cell disease. Sci. Transl. Med. *13*, eabf2444.

35. Paix, A., Folkmann, A., Goldman, D.H., Kulaga, H., Grzelak, M.J., Rasoloson, D., Paidemarry, S., Green, R., Reed, R.R., and Seydoux, G. (2017). Precision genome editing using synthesis-dependent repair of Cas9-induced DNA breaks. Proc. Natl. Acad. Sci. USA *114*, E10745–E10754.

36. Boontanrart, M.Y., Schröder, M.S., Stehli, G.M., Banović, M., Wyman, S.K., Lew, R.J., Bordi, M., Gowen, B.G., DeWitt, M.A., and Corn, J.E. (2020). ATF4 Regulates MYB to Increase γ-Globin in Response to Loss of β-Globin. Cell Rep. *32*, 107993.

37. Iancu, O., Allen, D., Knop, O., Zehavi, Y., Breier, D., Arbiv, A., Lev, A., Lee, Y.N., Beider, K., Nagler, A., et al. (2023). Multiplex HDR for disease and correction modeling of SCID by CRISPR genome editing in human HSPCs. Mol. Ther. Nucleic Acids *31*, 105–121.

38. Majeti, R., Park, C.Y., and Weissman, I.L. (2007). Identification of a hierarchy of multipotent hematopoietic progenitors in human cord blood. Cell Stem Cell *1*, 635–645.

39. Tomellini, E., Fares, I., Lehnertz, B., Chagraoui, J., Mayotte, N., MacRae, T., Bordeleau, M.È., Corneau, S., Bisaillon, R., and Sauvageau, G. (2019). Integrin-α3 Is a Functional Marker of Ex Vivo Expanded Human Long-Term Hematopoietic Stem Cells. Cell Rep. *28*, 1063–1073.e5.

40. Krebsbach, P.H., and Villa-Diaz, L.G. (2017). The Role of Integrin α6 (CD49f) in Stem Cells: More than a Conserved Biomarker. Stem Cells Dev. *26*, 1090–1099.

41. Shin, J.J., Schröder, M.S., Caiado, F., Wyman, S.K., Bray, N.L., Bordi, M., Dewitt, M.A., Vu, J.T., Kim, W.-T., Hockemeyer, D., et al. (2020). Controlled Cycling and Quiescence Enables Efficient HDR in Engraftment-Enriched Adult Hematopoietic Stem and Progenitor Cells. Cell Rep. *32*, 108093.

42. Kaufmann, K.B., Zeng, A.G.X., Coyaud, E., Garcia-Prat, L., Papalexi, E., Murison, A., Laurent, E.M.N., Chan-Seng-Yue, M., Gan, O.I., Pan, K., et al. (2021). A latent subset of human hematopoietic stem cells resists regenerative stress to preserve stemness. Nat. Immunol. *22*, 723–734.

43. Fares, I., Chagraoui, J., Lehnertz, B., MacRae, T., Mayotte, N., Tomellini, E., Aubert, L., Roux, P.P., and Sauvageau, G. (2017). EPCR expression marks UM171-expanded CD34+ cord blood stem cells. Blood *129*, 3344–3351.

44. Gomez-Ospina, N., Scharenberg, S.G., Mostrel, N., Bak, R.O., Mantri, S., Quadros, R.M., Gurumurthy, C.B., Lee, C., Bao, G., Suarez, C.J., et al. (2019). Human genome-edited hematopoietic stem cells phenotypically correct Mucopolysaccharidosis type I. Nat. Commun. *10*, 4045.

45. Schiroli, G., Conti, A., Ferrari, S., Della Volpe, L., Jacob, A., Albano, L., Beretta, S., Calabria, A., Vavassori, V., Gasparini, P., et al. (2019). Precise Gene Editing Preserves Hematopoietic Stem Cell Function following Transient p53-Mediated DNA Damage Response. Cell Stem Cell *24*, 551–565.e8.

46. Ferrari, S., Jacob, A., Cesana, D., Laugel, M., Beretta, S., Varesi, A., Unali, G., Conti, A., Canarutto, D., Albano, L., et al. (2022). Choice of template delivery mitigates the genotoxic risk and adverse impact of editing in human hematopoietic stem cells. Cell Stem Cell *29*, 1428–1444.e9.

47. Romero, Z., Lomova, A., Said, S., Miggelbrink, A., Kuo, C.Y., Campo-Fernandez, B., Hoban, M.D., Masiuk, K.E., Clark, D.N., Long, J., et al. (2019). Editing the sickle cell disease mutation in human hematopoietic stem cells: comparison of endonucleases and homologous donor templates. Mol. Ther. *27*, 1389–1406.

48. Magis, W., DeWitt, M.A., Wyman, S.K., Vu, J.T., Heo, S.-J., Shao, S.J., Hennig, F., Romero, Z.G., Campo-Fernandez, B., Said, S., et al. (2022). High-level correction of the sickle mutation is amplified in vivo during erythroid differentiation. iScience *25*, 104374.

49. Ferrari, S., Jacob, A., Beretta, S., Unali, G., Albano, L., Vavassori, V., Cittaro, D., Lazarevic, D., Brombin, C., Cugnata, F., et al. (2020). Efficient gene editing of human long-term hematopoietic stem cells validated by clonal tracking. Nat. Biotechnol. *38*, 1298–1308.

50. Ferrari, S., Beretta, S., Jacob, A., Cittaro, D., Albano, L., Merelli, I., Naldini, L., and Genovese, P. (2021). BAR-Seq clonal tracking of gene-edited cells. Nat. Protoc. *16*, 2991–3025.

51. Sharma, R., Dever, D.P., Lee, C.M., Azizi, A., Pan, Y., Camarena, J., Köhnke, T., Bao, G., Porteus, M.H., and Majeti, R. (2021). The TRACE-Seq method tracks recombination alleles and identifies clonal reconstitution dynamics of gene targeted human hematopoietic stem cells. Nat. Commun. *12*, 472.

52. Frangoul, H., Altshuler, D., Cappellini, M.D., Chen, Y.-S., Domm, J., Eustace, B.K., Foell, J., de la Fuente, J., Grupp, S., Handgretinger, R., et al. (2021). CRISPR-Cas9 Gene Editing for Sickle Cell Disease and β-Thalassemia. N. Engl. J. Med. *384*, 252–260.

53. Morgan, R.A., Unti, M.J., Aleshe, B., Brown, D., Osborne, K.S., Koziol, C., Ayoub, P.G., Smith, O.B., O'Brien, R., Tam, C., et al. (2020). Improved Titer and Gene Transfer by Lentiviral Vectors Using Novel, Small β-Globin Locus Control Region Elements. Mol. Ther. *28*, 328–340.

54. Wienert, B., Martyn, G.E., Funnell, A.P.W., Quinlan, K.G.R., and Crossley, M. (2018). Wake-up Sleepy Gene: Reactivating Fetal Globin for β-Hemoglobinopathies. Trends Genet. *34*, 927–940.

55. Everette, K.A., Newby, G.A., Levine, R.M., Mayberry, K., Jang, Y., Mayuranathan, T., Nimmagadda, N., Dempsey, E., Li, Y., Bhoopalan, S.V., et al. (2023). Ex vivo prime editing of patient haematopoietic stem cells rescues sickle-cell disease phenotypes after engraftment in mice. Nat. Biomed. Eng. *7*, 616–628.

56. Bauer, D.E., Kamran, S.C., Lessard, S., Xu, J., Fujiwara, Y., Lin, C., Shao, Z., Canver, M.C., Smith, E.C., Pinello, L., et al. (2013). An erythroid enhancer of BCL11A subject to genetic variation determines fetal hemoglobin level. Science *342*, 253–257.

57. Chu, S.H., Ortega, M., Feliciano, P., Winton, V., Xu, C., Haupt, D., McDonald, T., Martinez, S., Liquori, A., Marshall, J., et al. (2021). Conversion of HbS to Hb G-Makassar By Adenine Base Editing Is Compatible with Normal Hemoglobin Function. Blood *138*, 951.

58. Newby, G.A., Yen, J.S., Woodard, K.J., Mayuranathan, T., Lazzarotto, C.R., Li, Y., Sheppard-Tillman, H., Porter, S.N., Yao, Y., Mayberry, K., et al. (2021). Base editing of haematopoietic stem cells rescues sickle cell disease in mice. Nature *595*, 295–302.

59. Zhang, H., Sun, R., Fei, J., Chen, H., and Lu, D. (2022). Correction of Beta-Thalassemia IVS-II-654 Mutation in a Mouse Model Using Prime Editing. Int. J. Mol. Sci. *23*, 5948.

60. Akef, A., Lee, E.S., and Palazzo, A.F. (2015). Splicing promotes the nuclear export of β-globin mRNA by overcoming nuclear retention elements. RNA *21*, 1908–1920.

61. Kosicki, M., Tomberg, K., and Bradley, A. (2018). Repair of double-strand breaks induced by CRISPR-Cas9 leads to large deletions and complex rearrangements. Nat. Biotechnol. *36*, 765–771.

62. Adikusuma, F., Piltz, S., Corbett, M.A., Turvey, M., McColl, S.R., Helbig, K.J., Beard, M.R., Hughes, J., Pomerantz, R.T., and Thomas, P.Q. (2018). Large deletions induced by Cas9 cleavage. Nature *560*, E8–E9.

63. Park, S.H., Cao, M., Pan, Y., Davis, T.H., Saxena, L., Deshmukh, H., Fu, Y., Treangen, T., Sheehan, V.A., and Bao, G. (2022). Comprehensive analysis and accurate quantification of unintended large gene modifications induced by CRISPR-Cas9 gene editing. Sci. Adv. *8*, eabo7676.

64. Shyr, D.C., Lowsky, R., Miller, W., Schroeder, M.A., Buchholz, T., Dougall, K., Intondi, A., Charles, A., Lehrer, J., Bouge, A., et al. (2023). One Year Follow-up on the First Patient Treated with Nula-Cel: An Autologous CRISPR/Cas9 Gene Corrected CD34+ Cell Product to Treat Sickle Cell Disease. Blood *142*, 5000.

65. NIH VideoCast - Annual Sickle Cell Disease Meeting. https://videocast.nih.gov/watch=54991.

66. One Year Follow-up on the First Patient Treated with Nula-Cel. https://kamautx.com/wp-content/uploads/2023/12/ASH_poster_v3_1.pdf.

67. Perez-Bermejo, J.A., Efagene, O., Matern, W.M., Holden, J.K., Kabir, S., Chew, G.M., Andreoletti, G., Catton, E., Ennis, C.L., Garcia, A., et al. (2024). Functional screening in human HSPCs identifies optimized protein-based enhancers of Homology Directed Repair. Nat. Commun. *15*, 2625.

68. Baik, R., Cromer, M., Glenn, S., Vakulskas, C., Dudek, A., Feist, W., Shipp, S., Dever, D., and Porteus, M. (2023). Transient inhibition of 53BP1 increases the frequency of targeted integration in human hematopoietic stem and progenitor cells. Nat. Commun. *15*, 111.

69. Cullot, G., Aird, E.J., Schlapansky, M.F., Yeh, C.D., van de Venn, L., Vykhlyantseva, I., Kreutzer, S., Mailänder, D., Lewków, B., Klermund, J., et al. (2024). Genome editing with the HDR-enhancing DNA-PKcs inhibitor AZD7648 causes large-scale genomic alterations. Nat. Biotechnol. https://doi.org/10.1038/s41587-024-02488-6.

70. Dorset, S.R., and Bak, R.O. (2023). The p53 challenge of hematopoietic stem cell gene editing. Mol. Ther. Methods Clin. Dev. *30*, 83–89.

71. Frati, G., Brusson, M., Sartre, G., Mlayah, B., Felix, T., Chalumeau, A., Antoniou, P., Hardouin, G., Concordet, J.-P., Romano, O., et al. (2024). Safety and efficacy studies of CRISPR-Cas9 treatment of sickle cell disease highlights disease-specific responses. Mol. Ther. *32*, 4337–4352.

72. De Ravin, S.S., Brault, J., Meis, R.J., Liu, S., Li, L., Pavel-Dinu, M., Lazzarotto, C.R., Liu, T., Koontz, S.M., Choi, U., et al. (2021). Enhanced homology-directed repair for highly efficient gene editing in hematopoietic stem/progenitor cells. Blood *137*, 2598–2608.

73. Nagel, R.L., Fabry, M.E., and Steinberg, M.H. (2003). The paradox of hemoglobin SC disease. Blood Rev. *17*, 167–178.

74. Chagraoui, J., Girard, S., Spinella, J.-F., Simon, L., Bonneil, E., Mayotte, N., MacRae, T., Coulombe-Huntington, J., Bertomeu, T., Moison, C., et al. (2021). UM171 Preserves Epigenetic Marks that Are Reduced in Ex Vivo Culture of Human HSCs via Potentiation of the CLR3-KBTBD4 Complex. Cell Stem Cell *28*, 48–62.e6.